

Collisional Effects on Absorption and Energy Transport in a Dense Solid-Carbon Thin Film Irradiated by Subpicosecond Lasers

Mo CHEN, Daisuke SAITOU and Yasuaki KISHIMOTO

Graduate School of Energy Science, Kyoto University, Gokasyo, Uji, Kyoto 611-0011, Japan

(Received 8 June 2009 / Accepted 2 July 2009)

The collisional effects on the kinetics of interactions between a high-power subpicosecond laser and a solid-carbon thin film in a fast-ignition scenario are investigated by one-dimensional particle-in-cell simulations. Collisions are found to play an essential role in energy absorption and transport, compared to collisionless cases. In the collisional cases, the absorption at the heating edge, heat transport inside the thin film, and hot electron production are reduced in the early transient process.

© 2009 The Japan Society of Plasma Science and Nuclear Fusion Research

Keywords: high power laser-matter interaction, collisional effect, absorption rate, heat transport, fast ignition

DOI: 10.1585/pfr.4.040

In recent years, state-of-the-art lasers have developed rapidly with very short (subpicosecond) pulses and very high intensity (up to 10^{22} W/cm²), and are applied in many areas of science and technology, such as the fast ignition (FI) scheme of inertial confinement fusion (ICF) [1]. Unlike the case of long-pulse (nanosecond-order) lasers used in conventional ICF, which have been extendedly studied by more than 30 years [2], absorption and energy transport in short-pulse high-intensity laser-matter interaction in FI are unclear because of the sensitivity to the parameters of lasers and matter, such as the material's temperature, density, and ionization state, and laser intensity, wavelength, and duration [3–6]. Atomic processes, such as collision and ionization, play an important role in energy absorption, partition, and transport, which determine high-energy particle generation and ignition possibility.

To investigate collisional effects in a fully ionized solid-carbon thin film irradiated by a high-power subpicosecond laser pulse, we perform one-dimensional simulations using a particle-in-cell (PIC) code (EPIC3D) that includes collisional relaxation and ionization processes [7]. The size of the simulation box is $L_x = 13.12 \mu\text{m}$ (the normalized length is 1024Δ , and $\Delta = 1.28125 \times 10^{-2} \mu\text{m}$), where a step-like thin film is set in $200 \Delta < x < 700 \Delta$ ($6.4 \mu\text{m}$); its initial ion density is $5.6 \times 10^{22} \text{cm}^{-3}$ (half the solid carbon density) and the initial temperature is 0.511 keV. We turn the collision module on or off to compare the collisional and collisionless cases with the same simulation parameters. Collisional processes are modeled by the relativistic pairing method, which conserves energy and momentum precisely [8]. A p -polarized laser pulse without a prepulse with a Gaussian time profile is incident normally from the left side of the simulation box. The amplitude of the pulse rises for the first 30 fs to a max-

imum of 5.1×10^{19} W/cm² and maintains a semi-infinite envelope. The laser wavelength is $\lambda_L = 0.82 \mu\text{m}$, and the associated critical density is $1.7 \times 10^{21} \text{cm}^{-3}$. We set 320 particles per cell in the collisionless cases and 160 in the collisional cases, with 4096 meshes in either case, which assures the convergence of the simulations. Although the Debye length, $\lambda_D = 2.9 \times 10^{-4} \mu\text{m}$, is shorter than the mesh size, $\Delta x = (1/4)\Delta = 3.2 \times 10^{-3} \mu\text{m}$, in the high laser intensity regime, the temperature of the target increases quickly, and the Debye length also increases, which possibly avoids numerical heating effects.

The time histories of the electron, ion, field, and total energies are shown in Fig. 1 (a); the absorption (electron energy) is about 23% lower in the collisional case than in the collisionless case at $t = 128.2$ fs. The main absorption mechanism is considered to be $\mathbf{J} \times \mathbf{B}$ heating in the present laser intensity regime. The electron density and temperature for both cases are presented in Fig. 1 (b) at $t = 128.2$ fs. It is clear that in the collisional case, the temperature is higher with a steeper gradient in the heating region, and the heat front propagates more slowly with a smaller preheating foot than in the collisionless case, which shows that collisional effects strongly inhibit the early transient transport process. In addition, the spiky structure at two times the laser frequency due to p -polarized laser heating is inhibited in the collisional case [9]. In both cases, a density shock structure is generated at the front edge of the thin film after 30 fs, and evolves, as shown in Fig. 2. In the overdense region without photon pressure, a rarefaction wave develops and soon overtakes the shock to form a so-called blast wave; at the same time, the plasma expands into the left side and interacts with the photon pressure. In the collisional case, the shock dissipates more quickly than in the collisionless case. The dissipative mechanism is explained by ion heat conduction and ion viscosity due to col-

author's e-mail: mo@center.iae.kyoto-u.ac.jp

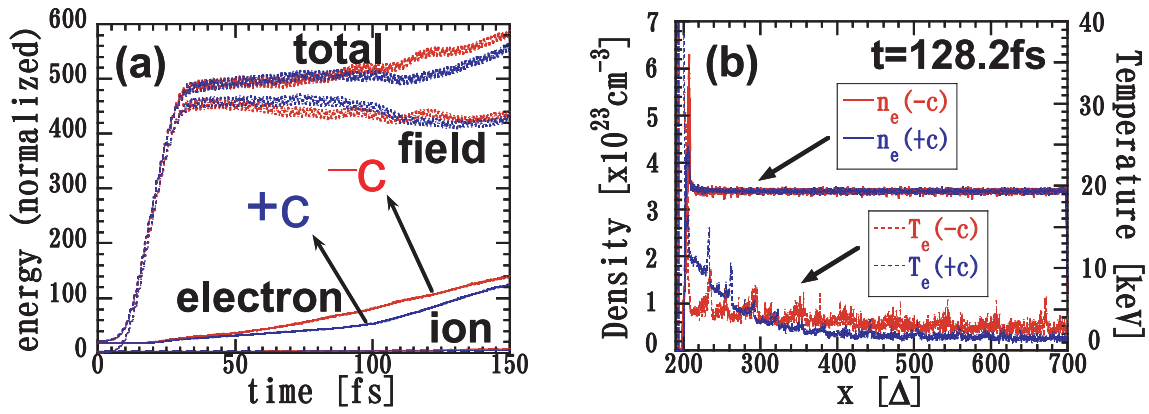


Fig. 1 (a) Time histories of electron, ion, field, and total energy for the collisional (“+c”) and collisionless (“-c”) cases and (b) electron density (n_e) and temperature (T_e) profiles at $t = 128.2$ fs.

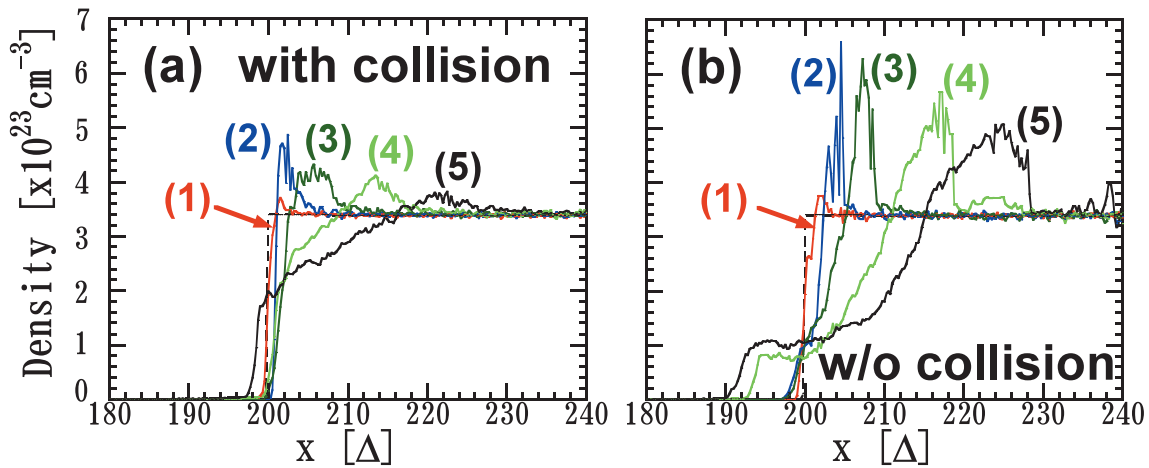


Fig. 2 Evolution of the density shock structure of electrons at times (1) 29.92 fs, (2) 64.11 fs, (3) 128.2 fs, (4) 256.4 fs, and (5) 384.6 fs. (a) is the collisional case and (b) is the collisionless case. The straight dashed line denotes the initial density of the thin film.

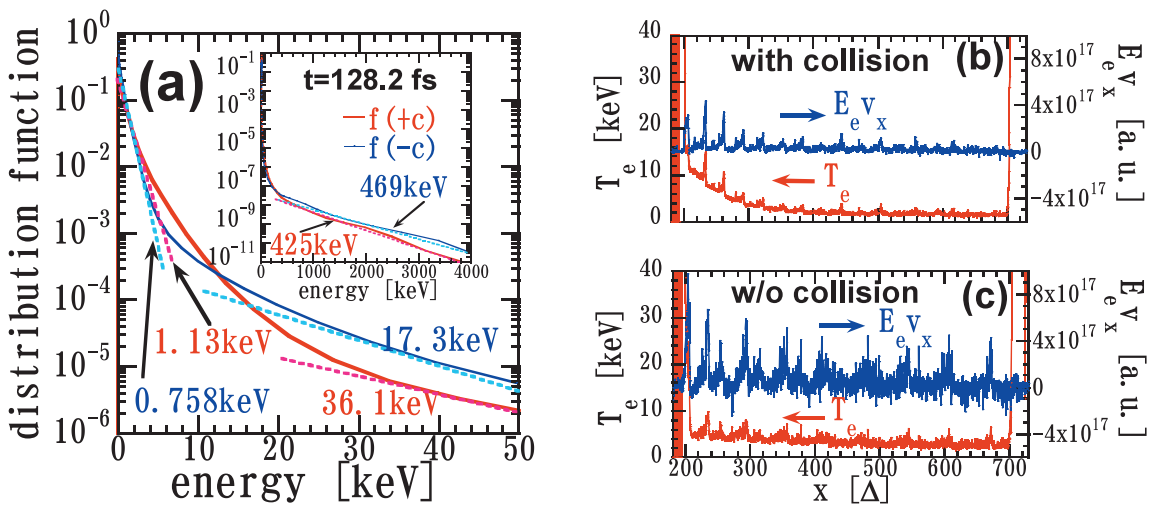


Fig. 3 (a) EDFs in energy space at $t = 128.2$ fs; the insets are the total EDFs, and the main panels are those in the low-energy region. Electron heat flux (denoted by $E_e v_x$) and temperature (denoted by T_e) profiles at $t = 128.2$ fs: (b) the collisional case and (c) the collisionless case.

lisional effects. In the collisional case, the photon pressure pushes the edge more so that the density gradient is steeper than in the collisionless case. In Fig. 1 (a), the difference in absorption between the two cases appears at $t = 30$ fs, when the density gradient becomes different consistently in Fig. 2. Other authors have shown that the steeper density gradient reduces the absorption rate by investigating different density scale lengths [10, 11]. Our simulations also present this absorption mechanism self-consistently due to the laser-produced density gradient.

The electron distribution functions (EDFs) integrated over the entire simulation box at $t = 128.2$ fs are displayed in Fig. 3 (a) for both cases. The characteristic features of three-sectional EDF are observed: bulk Maxwellian, non-local tail, and relativistic collisionless high-energy electrons. Comparing the equivalent temperatures of these three sections, we find that collisional effects with the present solid density parameter reduce the bulk temperature, preheating due to nonlocal electron transport, and hot electron production. In Figs. 3 (b) and (c), we also compare the heat flux in both cases and observe that the heat flux in the collisional case is about one order of magnitude less than that in the collisionless case, which directly proves heat transport inhibition.

The electron distribution in x - p_x phase space illustrates more details of the transport (the plots are omitted here due to limited space). Initially, the hot electrons are accelerated by the laser field. A return current of cold background electrons forms immediately to balance the hot electron current and provides resistive heating in the collisional case. At the early time $t < 60$ fs, the main transport mechanism is resistive heating due to collisions. When they reach the rear side of the thin film, the hot electrons

are reflected by the strong sheath field, and recirculation occurs. The return current of reflected hot electrons suppresses the cold electron return current and affects the later energy transport. In the collisionless case, similar processes occur except for the resistive heating. Without the drag force, the hot electrons have larger velocities, and collisionless transport with recirculation plays a major role. When the entire thin film is heated after around 300 fs, the collisionality is reduced because of the high temperature, and the differences between the two cases become smaller.

In conclusion, the collisional effects on absorption and energy transport in interactions between a subpicosecond high-power laser and an overdense carbon thin film are studied by a 1D PIC code with a collisional relaxation module. Collisions between hot and cold electrons reduce the absorption at the heating edge, heat transport inside the thin film, and hot electron production, which may affect the energy deposition and ignition possibility in FI.

- [1] M. Tabak *et al.*, Phys. Plasmas **1**, 1626 (1994).
- [2] J.D. Lindl *et al.*, Phys. Plasmas **11**, 339 (2004).
- [3] J.R. Davies, Plasma Phys. Control. Fusion **51**, 014006 (2009).
- [4] A.R. Bell *et al.*, Plasma Phys. Control. Fusion **48**, R37 (2006).
- [5] S.M. Guérin *et al.*, Plasma Phys. Control. Fusion **41**, 285 (1999).
- [6] J. Denavit, Phys. Rev. Lett. **69**, 3052 (1992).
- [7] T. Masaki and Y. Kishimoto, J. Plasma Phys. **72**, 1291 (2006).
- [8] Y. Sentoku *et al.*, J. Phys. Soc. Jpn. **67**, 4084 (1998).
- [9] R. Lichters *et al.*, Phys. Plasmas **3**, 3425 (1996).
- [10] A.J. Kemp *et al.*, Phys. Rev. Lett. **101**, 075004 (2008).
- [11] S.C. Wilks, Phys. Fluids B **5**, 2603 (1993).